Numerical Simulation of Convex Shape Beam Spot on Stress Field of Plasma-sprayed MCrAlY Coating During Laser Cladding Process

Peipei Zhang
Tongling University
Jiaqing Chu
Tongling University
Guang Qu
Tongling University
Dongsheng Wang (wangdongsheng@tlu.edu.cn)
Tongling University

Research Article

Keywords: Laser cladding, Numerical simulation, Thermal stress, Convex shape beam spot, Uniform rectangular beam spot

Posted Date: March 5th, 2021

DOI: https://doi.org/10.21203/rs.3.rs-274842/v1

Version of Record: A version of this preprint was published at The International Journal of Advanced Manufacturing Technology on September 3rd, 2021. See the published version at https://doi.org/10.1007/s00170-021-07949-9.

Abstract

In order to reduce the thermal stress at clad layer and further reduce the crack generation in the laser cladding process, a method of controlling the cracks at clad layer by changing the laser energy density was proposed. The comparative thermal-mechanical coupling finite element analysis was conducted for the uniform rectangular spot and convex shape beam spot cladding processes on plasma-sprayed MCrAlY coating through the numerical simulation method based on the ANSYS software. The results show that the rapid heating and cooling characteristics, which are typical in laser processing, are manifested in the cladding process using the uniform rectangular spot, and the convex shape spot can exert the preheating and slow cooling effects to a certain extent, so as to reduce the temperature gradient of the cladding zone and non-cladding zone. In addition, on the precondition of equivalent cladding effect, the thermal stress at the clad layer is also low, so the cracking tendency of the clad layer can be effectively mitigated. Relative to the laser beam shaped diffractive optical element special for design and manufacturing, superposing two uniform rectangular spots with different sizes and energy densities is a simpler and more effective method of acquiring the convex shape spot.

1. Introduction

Laser cladding refers to radiating high-energy-density laser beams on the surface of base material and forming a layer of materials with special physical, chemical or mechanical properties on it through rapid melting, expansion and solidification. In comparison with other surface machining technologies, the laser cladding technology integrates the merits of broad scope of application, strong practicability and flexible application, so it has aroused extensive attention and attracted great importance and has been widely used [1-8]. At present the major problem in laser cladding is high coating brittleness and great cracking tendency [9-16], which considerably restricts its scope of application in key components, so cracking inhibition in the laser cladding is of great realistic significance to the application of the laser cladding technology in production.

The main methods of inhibiting cracking of clad layer at present include: adjust the stress state and reduce the tensile stress as much as possible [17-19]; optimize the process method and parameters [20-29]; reasonably design the clad layer [29-34] and change the laser action mode [35, 36], etc. From the angle of cladding material, laser cladding nano coating can effectively solve the easy cracking problem of clad layer by virtue of strong toughening effect of nanomaterial [29]. The measure commonly used to adjust the stress state at the clad layer is preheating and/or cold treatment of the specimen. For instance, Literature [17] investigated the influence of substrate preheating on laser cladding, and conducted the laser cladding tests at different preheating temperatures, and the results showed that the laser cladding under substrate preheating condition could significantly improve the specimen mass, effectively reduce the thermal stress in the cladding process, and reduce the crack generation at the clad layer. The composite laser cladding technology is also one of the effective methods of controlling the cracks at clad layer. Literatures [20-28] combined induction heater [20-24], ultrasonic vibration [25], electromagnetic field

[26], alternating current electric field [27] and pulsed current [28] et al. with laser cladding, thus controlling the crack formation at the clad layer very well.

The essence of preheating and/or slow cooling treatment lies in reducing the temperature gradient in the laser cladding process. In fact, the solidification of clad layer is an extremely fast process after laser cladding, and the process from stress generation to stress concentration until crack formation is also very fast. Therefore, the preheating and/or slow cooling treatment should run through the whole laser cladding process in order to give full play to the effects of preheating and slow cooling treatment on improving the quality of clad layer or eliminating the crack generation. This problem can be well solved using the incubator dedicated for laser cladding. However, on the one hand, the incubator should synchronously operate with laser cladding, and on the other hand, different incubators should be designed for different specimens, which brings about a certain difficulty to the laser processing operation and incubator design, specially to overall heating and heat insulation of large specimens. In Literature [24], the induction heating method was used to realize local preheating of the specimen and reached favorable effect. This method could not only greatly improve the cladding efficiency but also acquired a crack-free clad layer, and meanwhile, but the complexity of the whole system was aggravated by the added heat source. Shang et al. [36] pointed out that the laser cladding NiCrBSi structure could be effectively controlled by changing the energy density of circular laser beam.

Enlightened by the methods of preheating and slow cooling treatment and changing the energy density of laser beam, if the laser is properly transformed, the energy density distribution of uniform rectangular spot commonly used in laser cladding can be changed to acquire the convex shape spot with high energy density distribution in middle and low energy density distribution at edges along the laser scanning direction. During the laser cladding process, the specimen can be preheated at front end of the spot, the cladding treatment is carried out in the central high-energy-density zone, while the cooling speed of clad layer can be slowed down at rear end of the spot. In this way, no additional device is needed, and meanwhile, the effect similar to preheating and slow cooling can be reached, so as to reduce the temperature gradient of laser cladding zone and non-laser cladding zone, and mitigate the cracking tendency at clad layer. The thermal-mechanical coupling finite element numerical simulation was conducted for the laser cladding process on plasma-sprayed MCrAlY coating with the spot presenting uniform rectangular energy density distribution and those presenting convex shape energy density distribution via the ANSYS software, in an effort to investigate the influences of convex shape spot on the specimen preheating and slow cooling effect of laser cladding and the stress, and verify its effectiveness in controlling the cracks at clad layer. After then, the implementation method of the convex shape spot was discussed.

2. Thermal-mechanical Coupling Finite Element Modeling

The substrate material was γ-TiAl based alloy (TAC-2) smelted by Institute of High-Temperature Materials, Central Iron and Steel Research Institute, the MCrAlY coating was prepared through the plasma spraying process using the Y_2O_3-strengthened high-temperature alloy composite powder NiCoCrAl (KF-113A)

produced by Institute of Metal Materials, Beijing General Research Institute of Mining and Metallurgy. The substrate dimensions of the specimen were 30 mm×20 mm×5 mm, the thickness of the coating was 0.15 mm, and one half of the specimen, which was symmetric with the center line of laser scanning as shown in Fig. 1.

The main models used to describe laser heat source include Rosonthal analytical model, Gauss distribution heat source model, uniform heat source model, semispherical heat source model, ellipsoidal model and double-ellipsoid heat source model [37-50], etc. As for laser cladding, diffractive optical element is usually used to transform Gauss beam into rectangular beam with uniform energy density distribution [51], so the uniform heat source model is usually applied in numerical simulation.

Two laser heat source models are used in the numerical simulation: uniform rectangular spot, with concrete parameters as follows: laser power of 950 W, spot size of 5 mm×3 mm, laser scanning direction of along 3 mm side of the spot, and scanning speed of 600 $mm \cdot min^{-1}$; convex shape spot (superposed by two uniform rectangular spots with the same center but different sizes), namely one uniform small rectangular spot with laser power of 675 W and size of 5 mm×3 mm, and one uniform large rectangular spot with laser power of 675 W and size of 5 mm×15 mm, the scanning direction is along the 3/15 mm side of the spot, and the scanning speed is 600 $mm \cdot min^{-1}$. The energy density distributions of the two spots are shown in Fig. 2.

The corresponding finite element numerical simulation model was established through the indirect thermal-mechanical coupling method via the ANSYS finite element software, and the concrete model construction is seen in Literatures [52,53] in details.

3. Model Calculation Results And Discussion

Fig. 3 displays the temperature field nephogram at 1.5 s of laser scanning under two process parameters, where the zone with the temperature higher than 1,460 ^{o}C (melting point of TiAl alloy) in the Fig. 3 is molten pool zone. It can be seen from the Fig. 3 that in comparison with the uniform rectangular spot, the isothermal zone cladded using convex shape spot is large, in other words, the temperature gradient of cladding zone and non-cladding zone is small.

The cross-sectional temperature field nephogram at the maximum temperature point at 1.5 s is shown in Fig. 4, and the isothermal line presents crescent shape. The substrate melting depth and interfacial metallurgical bonding breadth can be judged according to the 1,460 ^{o}C isothermal line. When the uniform rectangular spot is used, the interfacial metallurgical bonding breadth and substrate melting depth are 3.04 mm and 134 μm, respectively, and those when the convex shape spot is used are 3.03 mm and 145 μm, respectively, so they achieve equivalent cladding effect on the whole. It can be seen by comparing the two figures that the maximum temperatures achieved by using the uniform rectangular spot and convex shape spot are 1,906 ^{o}C and 1,820 ^{o}C, where the latter is slightly lower than the former, but as the convex shape spot is relatively larger, the laser irradiation time is longer, so is the existence time of molten pool,

and thus more heat quantity can be transferred towards the depth direction. Moreover, the temperature gradient is small in the depth direction, the practical cladding effects of the two process parameters are equivalent, and only that the ratio of substrate melting depth to interfacial metallurgical bonding breadth is relatively higher when the convex shape spot is used in the cladding process.

The temperature cyclic curve at the midpoint of center line on upper surface of the specimen is shown in Fig. 5. It can be seen that when the uniform rectangular spot is used for cladding, the temperature at the spot is slowly rising before the laser beam scans to this spot; when the laser beam scans to this point, the temperature will be rapidly increased to high temperature, and then rapidly cooled as the laser leaves, so rapid heating and rapid cooling characteristics, which are typical in laser machining, are presented. During the cladding process using convex shape spot, the temperature cyclic curve at this point is similar to the laser spot shape, namely convex shape, and at the front end is equal to local preheating of the specimen at 400 ^{o}C. However, influenced by the laser heat action, the temperature is relatively high in the cooling phase, presenting incompletely symmetric distribution. In general, when the convex shape spot is used, the temperature gradient is small no matter at front end or rear end of laser cladding, obvious preheating and slow cooling features are manifested, and this can relieve the adverse effect of fast heating and fast cooling in laser cladding on coating stress to some extent.

The early-stage research indicates that the tensile stress of the laser cladding specimen is the maximum along the laser scanning direction (transverse) [53], and high tensile stress is closely related to the crack formation at clad layer. Therefore, the influences of only the two spots on transverse stress in the cladding process will be discussed in this paper. Fig. 6 shows the transverse stress cyclic curve at the midpoint of the laser scanning center line on the upper surface of the specimen. It can be observed that before and after the molten pool is formed, the compressive stresses are equivalent under the two process conditions, but in terms of the tensile stress playing a significant role in the crack formation at clad layer, the tensile stress formed by using the convex shape spot is obviously lower than that using the uniform rectangular spot in the subsequent cooling process. According to the calculation results, as the cooling proceeds till 300 s, the tensile stress (may be considered as residual stress) of the uniform rectangular spot is 397.66 MPa, while that of the convex shape spot is 355.83 MPa, which is reduced by 10.5% comparatively.

The transverse stress distribution on the laser scanning center line on the upper surface of the specimen at 300 s is presented in Fig. 7. It can be clearly seen that the residual stress distributions under the two process conditions are similar: The transverse stress on the center line of the whole workpiece is tensile stress, the stress is rapidly increased at the initial end of laser scanning, and this very high stress level is kept in the central area until the end point of laser scanning. However, the residual stress of the convex shape spot is lower than that of the uniform rectangular spot, averagely by about 40 MPa in the central area. Through the previous numerical simulation, it is theoretically proved that the convex shape spot is effective for controlling the crack generation in the laser cladding process.

4. Implementation Method Of Convex Shape Beam Spot

The convex shape laser spot can be implemented by two methods: (1) The diffractive optical element can transform Gauss laser into a rectangular spot with uniform energy density, or other laser beams presenting any power density distribution. Therefore, the special diffractive optical element outputting convex shape spot can be directly manufactured through the laser beam shaped diffractive optical element design. However, on the one hand, the design and manufacturing of special diffractive optical element outputting convex shape spot can be complicated, and on the other hand, it is not convenient to adjust the convex shape spot output by the well designed special diffractive optical element. (2) The universal diffractive optical element, which can transform Gauss beam into uniform rectangular beam, can be used to generate the convex shape spot by superposing two uniform rectangular spots with different sizes and energy densities. Fig. 8 is a schematic diagram of convex shape beam spot generation through double-beam superposition of uniform rectangular beam spot.

For the superposition of two uniform rectangular laser beams, the preheating and slow cooling effects of the convex shape spot can be conveniently adjusted by controlling the power of two laser beams, spot size and central position of the spot. For example, when the center of the rectangular spot with large size and low energy density along the scanning direction is located at the front end of the rectangular spot with small size and high energy density, the preheating time will be longer than the slow cooling time, and the preheating effect is superior to the slow cooling effect; on the contrary, if the center of the rectangular spot with large size and low energy density along the scanning direction is located at the rear end of the rectangular spot with small size and high energy density, the slow cooling time is longer than the preheating time, and the slow cooling effect is better than the preheating effect. If the laser scanning speed and power remain unchanged while the size of large spot is reduced, the energy density will increase, the preheating and slow cooling temperatures will rise, but the preheating and slow cooling time will be shortened. Hence, the too small size of large spot will result in insufficient preheating and slow cooling time, with limited effect on reducing the residual stress at the clad layer; when the size of large spot is enlarged, the preheating and slow cooling time can be lengthened, but meanwhile, the reduction of energy density will bring about the reduction of preheating and slow cooling temperatures. Given this, the too large size of large spot will give rise to insufficient preheating and slow cooling temperatures and this is not good for reducing the residual stress at the clad layer.

From the previous analysis, for the implementation of convex shape spot through double-beam superposition, the power of two uniform rectangular laser beams, spot size and spot action center will exert great influences on the preheating and slow cooling of the clay layer, thus directly deciding the crack controlling effect, so the convex shape beam remains to be further optimized in the follow-up research.

For the crack controlling method by changing the laser energy density distribution (convex shape spot is used), the crack controlling of the clad layer is synchronously implemented with laser cladding, which is its advantage; in addition, the local heating treatment consumes less energy; especially, it can realize the effects similar to preheating and slow cooling without needing any additional device, the implementation and control are quite simple, so it is a convenient and feasible crack controlling measure for the clad layer. Relative to the special diffractive optical element outputting the convex shape beam, when the

superposition method of the double uniform rectangular beams is superposed, the preheating and slow cooling effects of the convex shape spot can be conveniently controlled by regulating the powers, spot sizes and action centers of the two uniform rectangular spots respectively in the convex shape spot, so it is a simpler and more effective method.

5. Conclusion

(1)The crack control method for the clad layer by changing the laser energy density distribution was proposed in this study. The effectiveness of laser cladding on plasma-sprayed MCrAlY coating with the laser spot presenting convex shape energy density distribution in reducing the thermal stress at the clad layer and relieving the crack generation was verified through the numerical simulation method based on the ANSYS finite element software.

(2)The numerical simulation results indicate that in comparison with the uniform rectangular laser spot, the laser cladding with the convex shape spot exerts the preheating and slow cooling effects to some extent, thus reducing the temperature gradient of laser cladding zone and non-cladding zone. Given the given parameters, the thermal stress can be reduced by over 10%.

(3)Relative to the laser beam shaped diffractive optical element specialized for the design and manufacturing, the superposition of two uniform rectangular beam spots with different sizes and energy densities is a simpler and more effective method of acquiring the convex shape beam spot.

Declarations

Ethical Approval

Ethics approval was not required for this research.

Consent to Participate

Consent to Participate was not required for this research.

Consent to Publish

All the authors agreed to publish the manuscript.

Authors Contributions

Methodology, Peipei Zhang and Dongsheng Wang; data curation, Jiaqing Chu and Guang Qu; writing—original draft preparation, Peipei Zhang and Dongsheng Wang.

Funding

We would like to express our sincere thanks to the Anhui Provincial Natural Science Foundation (Grant No. 2008085ME149), Anhui Provincial Top Academic Aid Program for Discipline (Major) Talents of Higher Education Institutions (Grant No. gxbjZD2020087), Anhui Provincial Natural Science Research Key Program of Higher Education Institutions (Grant No. KJ2020A0693, KJ2020A0700, KJ2018A0479, KJ2015A197), Key Research and Development Project of Tongling City (Grant No. 20200201010), Anhui Provincial Excellent Young Talents Fund Key Program of Higher Education Institutions (Grant No. gxyqZD2016320), Anhui Provincial Excellent Young Talents Fund Domestic Visiting and Study Program of Higher Education Institutions (Grant No. gxgnfx2020101), Major Key Project of Tongling University (Grant No.2020tlxyxs) and Anhui Provincial University Student Innovation and Entrepreneurship Training Programs (Grant No. s202010383305).

Competing Interests

The authors declare no conflict of interest.

Availability of data and materials

Not applicable.

References

1. Jeyaprakash N, Yang CH, Tseng SP (2020) Characterization and tribological evaluation of NiCrMoNb and NiCrBSiC laser cladding on near-α titanium alloy. Int J Adv Manuf Technol 106: 2347–2361
2. Lian G, Xiao S, Zhang Y,Jiang J, Zhan Y (2021) Multi-objective optimization of coating properties and cladding efficiency in 316L/WC composite laser cladding based on grey relational analysis. Int J Adv Manuf Technol 112: 1449–1459
3. Adesina OS, Popoola API, Pityana SL,Oloruntoba DT. (2018) Microstructural and tribological behavior of in situ synthesized Ti/Co coatings on Ti-6Al-4V alloy using laser surface cladding technique. Int J Adv Manuf Technol 95: 1265–1280
4. Singh S, Goyal DK, Kumar P, Bansal A (2020) Laser cladding technique for erosive wear applications: a review. Mater Res Express 7: 012007
5. Quazi MM, Fazal MA, Haseeb ASMA, Yusof F, Masjuki HH, Arslan A (2016) A review to the laser cladding of self-lubricating composite coatings. Lasers Manuf Mater Process 3: 67–99
6. Santo L (2008) Laser cladding of metals: a review. Int J Surf Sci Eng 2: 327–336
7. Weng F, Chen C, Yu H (2014) Research status of laser cladding on titanium and its alloys: A review. Mater Des 58: 412–425
8. Aghili SE, Shamanian M (2019) Investigation of powder fed laser cladding of NiCr-chromium carbides single-tracks on titanium aluminide substrate. Opt Laser Technol 119: 105652
9. Nazemi N, Urbanic J. Alam M (2017) Hardness and residual stress modeling of powder injection laser cladding of P420 coating on AISI 1018 substrate. Int J Adv Manuf Technol 93:3485–3503

10. Köhler H, Partes K, Kornmeier JR, Vollertsen F (2012) Residual stresses in steel specimens induced by laser cladding and their effect on fatigue strength. Phys Procedia 39 354–361
11. Fu F, Zhang Y, Chang G, Dai J (2016) Analysis on the physical mechanism of laser cladding crack and its influence factors. Optik 127: 200–202
12. Wang A, Fan C, Xie C, Huang W, Cui K (1996) Laser cladding of iron-base alloy on Al-Si alloy and its relation to cracking at the interface. J Mater Eng Perform 5: 775–783
13. He B, Li D, Zhang A, Lu Z, Ge J, Khoa DT (2013) Influence of oxidation on the cracks of DZ125L nickel-based superalloy thin-walled parts in laser metal direct forming. Rapid Prototyp J 19: 446–451
14. Wang F, Mao H, Zhang D, Zhao X, Shen Y. (2008) Online study of cracks during laser cladding process based on acoustic emission technique and finite element analysis. Appl Surf Sci 255: 3267–3275
15. Lee C, Park H, Yoo J, Lee C, Woo WC, Park S (2015) Residual stress and crack initiation in laser clad composite layer with Co-based alloy and WC+ NiCr. Appl Surf Sci 345: 286–294
16. Wang J, Li L, Tao W (2016) Crack initiation and propagation behavior of WC particles reinforced Fe-based metal matrix composite produced by laser melting deposition. Opt Laser Technol 82: 170–182
17. [17] Ding C, Cui X, Jiao J, Zhu P (2018) Effects of substrate preheating temperatures on the microstructure, properties, and residual stress of 12CrNi2 prepared by laser cladding deposition technique. Materials 11: 2401
18. [18] Wang F, Mao H, Zhang D, Zhang X (2009) The crack control during laser cladding by adding the stainless steel net in the coating. Appl Surf Sci 255: 6646–6654
19. [19] Li G J, Li J, Luo X (2015) Effects of post-heat treatment on microstructure and properties of laser cladded composite coatings on titanium alloy substrate. Opt Laser Technol 65: 66–75
20. Farahmand P, Kovacevic R (2015) Laser cladding assisted with an induction heater (LCAIH) of Ni-60% WC coating. J Mater Process Technol 222: 244–258
21. Farahmand P, Liu S, Zhang Z, Kovacevic R (2014) Laser cladding assisted by induction heating of Ni-WC composite enhanced by nano-WC and La_2O_3. Ceram Int 40: 15421–15438
22. Zhou S, Lei J, Dai X, Guo J, Gu Z, Pan H (2016) A comparative study of the structure and wear resistance of NiCrBSi/50 wt.% WC composite coatings by laser cladding and laser induction hybrid cladding. Int J Refract Met Hard Mater 60: 17–27
23. Wang D, Hu Q, Zeng X (2015) Residual stress and cracking behaviors of $Cr_{13}Ni_5Si_2$ based composite coatings prepared by laser-induction hybrid cladding. Coat Technol 274: 51–59
24. Zhou S, Zeng X, Hu Q, Huang Y (2008) Analysis of crack behavior for Ni-based WC composite coatings by laser cladding and crack-free realization. Appl Surf Sci 255: 1646–1653
25. Li M, Zhang Q, Han B, Song L, Cui G, Yang J, Li J (2020) Microstructure and property of Ni/WC/La_2O_3 coatings by ultrasonic vibration-assisted laser cladding treatment. Opt Lasers Eng 125: 105848
26. Zhai LL, Ban CY, Zhang JW (2019) Investigation on laser cladding Ni-base coating assisted by electromagnetic field. Opt Laser Technol 114: 81–88

27. Zhai L, Wang Q, Zhang J, Ban C (2019) Effect of alternating current electric field on microstructure and properties of laser cladding Ni-Cr-B-Si coating. Ceram Int 45: 16873–16879
28. Xie D, Zhao J, Qi Y, Li Y, Shen L, Xiao M (2013) Decreasing pores in a laser cladding layer with pulsed current. Chin Opt Lett 11: 111401
29. Xie S, Li R, Yuan T, Chen C, Zhou K, Song B, Shi Y (2018) Laser cladding assisted by friction stir processing for preparation of deformed crack-free Ni-Cr-Fe coating with nanostructure. Opt Laser Technol 99: 374–381
30. Lu Y, Huang G, Wang Y, Li H, Qin Z, Lu X (2018) Crack-free Fe-based amorphous coating synthesized by laser cladding. Mater Lett 210: 46–50
31. Abioye TE, McCartney DG, Clare AT (2015) Laser cladding of Inconel 625 wire for corrosion protection. J Mater Process Technol 217: 232–240
32. Amado JM, Tobar MJ, Yáñez A, Amigó V, Candel JJ (2011) Crack free tungsten carbide reinforced Ni (Cr) layers obtained by laser cladding. Phys Procedia 12: 338–344
33. Luo X, Li J, Li G J (2015) Effect of NiCrBSi content on microstructural evolution, cracking susceptibility and wear behaviors of laser cladding WC/Ni–NiCrBSi composite coatings. J Alloys Compd 626: 102–111
34. Lee C, Park H, Lee C (2014) Cracking susceptibility of laser cladding process with Co-based metal matrix composite powders. J Weld. Joining 32: 577–582
35. Farnia A, Ghaini FM, Ocelík V, Hosson JThMDe (2013) Microstructural characterization of Co-based coating deposited by low power pulse laser cladding. J Mater Sci 48: 2714–2723
36. Shang S, Wellburn D, Sun YZ, Wang SY, Chen J, Liang J, Liu CS (2014) Laser beam profile modulation for microstructure control in laser cladding of an NiCrBSi alloy. Surf Coat Technol 248: 46–53
37. Zhang Z, Kovacevic R (2019) A thermo-mechanical model for simulating the temperature and stress distribution during laser cladding process. Int J Adv Manuf Technol 102:457–472
38. Javid Y, Ghoreishi M (2017) Thermo-mechanical analysis in pulsed laser cladding of WC powder on Inconel 718. Int J Adv Manuf Technol 92:69–79
39. Liu H, Li M, Qin X,Huang S, Hong F (2019) Numerical simulation and experimental analysis of wide-beam laser cladding. Int J Adv Manuf Technol 100, 237–249
40. Liu H, Qin X, Wu M,Ni M, Huang S (2019) Numerical simulation of thermal and stress field of single track cladding in wide-beam laser cladding. Int J Adv Manuf Technol 104: 3959–3976
41. Tamanna N, Crouch R, Naher S (2019) Progress in numerical simulation of the laser cladding process. Opt Lasers Eng 122: 151–163
42. Raju R, Petley V, Duraiselvam M, Verma S, Rajendran R (2014) Numerical finite element investigation on laser cladding of aerospace components. Life Cycle Reliab Saf Eng 3: 13–23
43. Lee YS, Zhang W (2016) Modeling of heat transfer, fluid flow and solidification microstructure of nickel-base superalloy fabricated by laser powder bed fusion. Addit Manuf 12: 178–188

44. Masoomi M, Thompson SM, Shamsaei N (2017) Laser powder bed fusion of Ti-6Al-4V parts: Thermal modeling and mechanical implications. Int J Mach Tools Manuf 118–119: 73–90
45. Nazemi N, Urbanic RJ (2018) A numerical investigation for alternative toolpath deposition solutions for surface cladding of stainless steel P420 powder on AISI 1018 steel substrate. Int J Adv Manuf Technol 96: 4123–4143
46. Tseng WC, Aoh JN (2013) Simulation study on laser cladding on preplaced powder layer with a tailored laser heat source. Opt Laser Technol 48: 141–152
47. Hao M, Sun YA (2013) FEM model for simulating temperature field in coaxial laser cladding of Ti6Al4V alloy using an inverse modeling approach. Int J Heat Mass Transfer 64: 352–360
48. Gan Z, Yu G, He X, Li S (2017) Numerical simulation of thermal behavior and multicomponent mass transfer in direct laser deposition of Co-base alloy on steel. Int JHeat Mass Transfer 104: 28–38
49. Jendrzejewski R, Śliwiński G, Krawczuk M, Ostachowicz W (2004) Temperature and stress fields induced during laser cladding. Comput Struct 82: 653–658
50. Lei Y, Sun R, Tang Y, Niu W (2012) Numerical simulation of temperature distribution and TiC growth kinetics for high power laser clad TiC/NiCrBSiC composite coatings. Opt Laser Technol 44: 1141–1147
51. Liu H, Qin X, Huang S, Hu Z, Ni M (2018) Geometry modeling of single track cladding deposited by high power diode laser with rectangular beam spot. Opt Lasers Eng 100: 38–46
52. Wang D, Yue L, Yang H, Zhang P (2021) Computational analysis of laser cladding of preset MCrAlY coating based on ANSYS I–Temperature field. Mater Sci Forum 1020: 139–147
53. Wang D, Yang K, Yang H, Zhang P (2021) Computational analysis of laser cladding of preset MCrAlY coating based on ANSYS II–Stress field. Mater Sci Forum 1020: 148–156

Figures

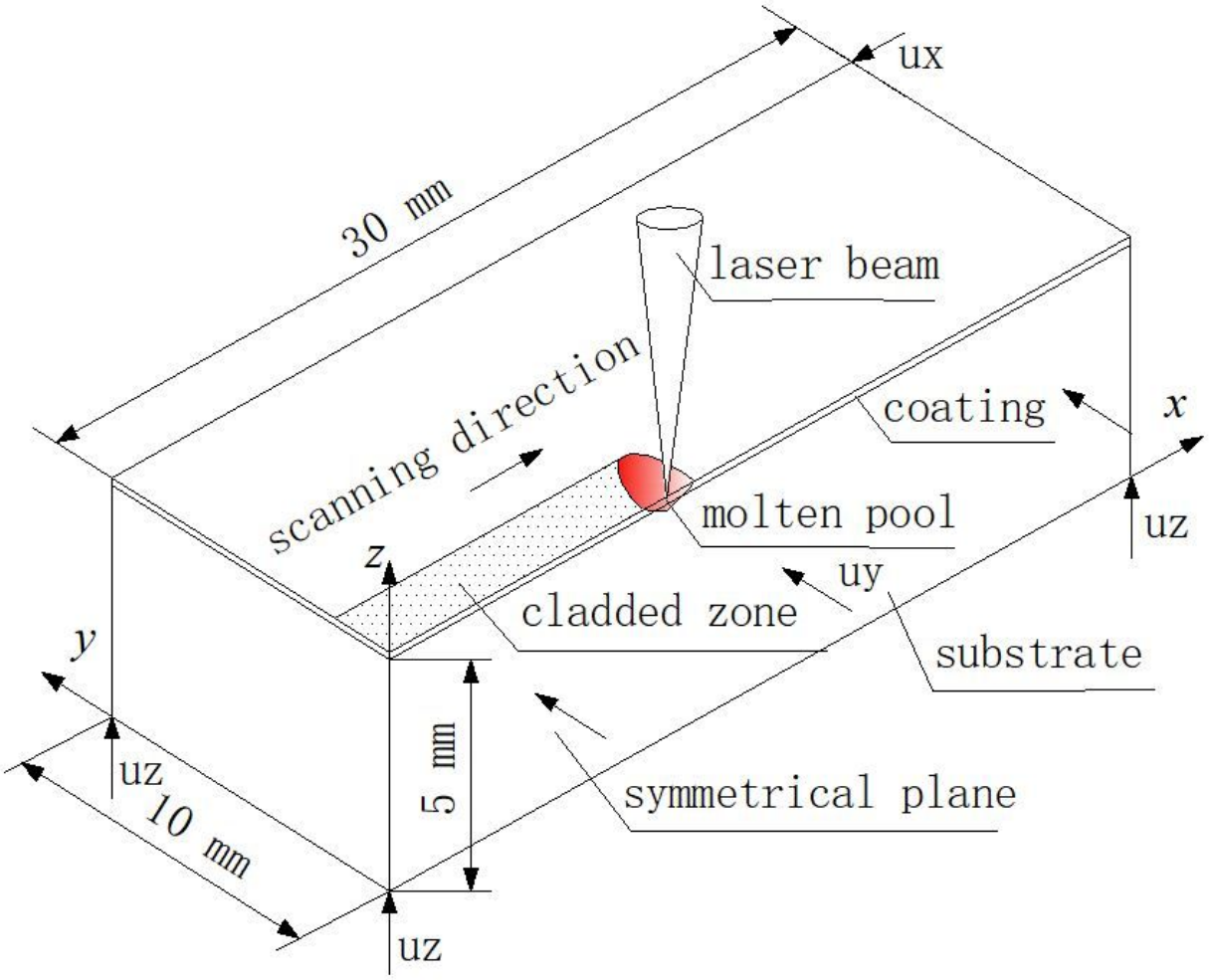

Figure 1

Schematic diagram of laser cladding process

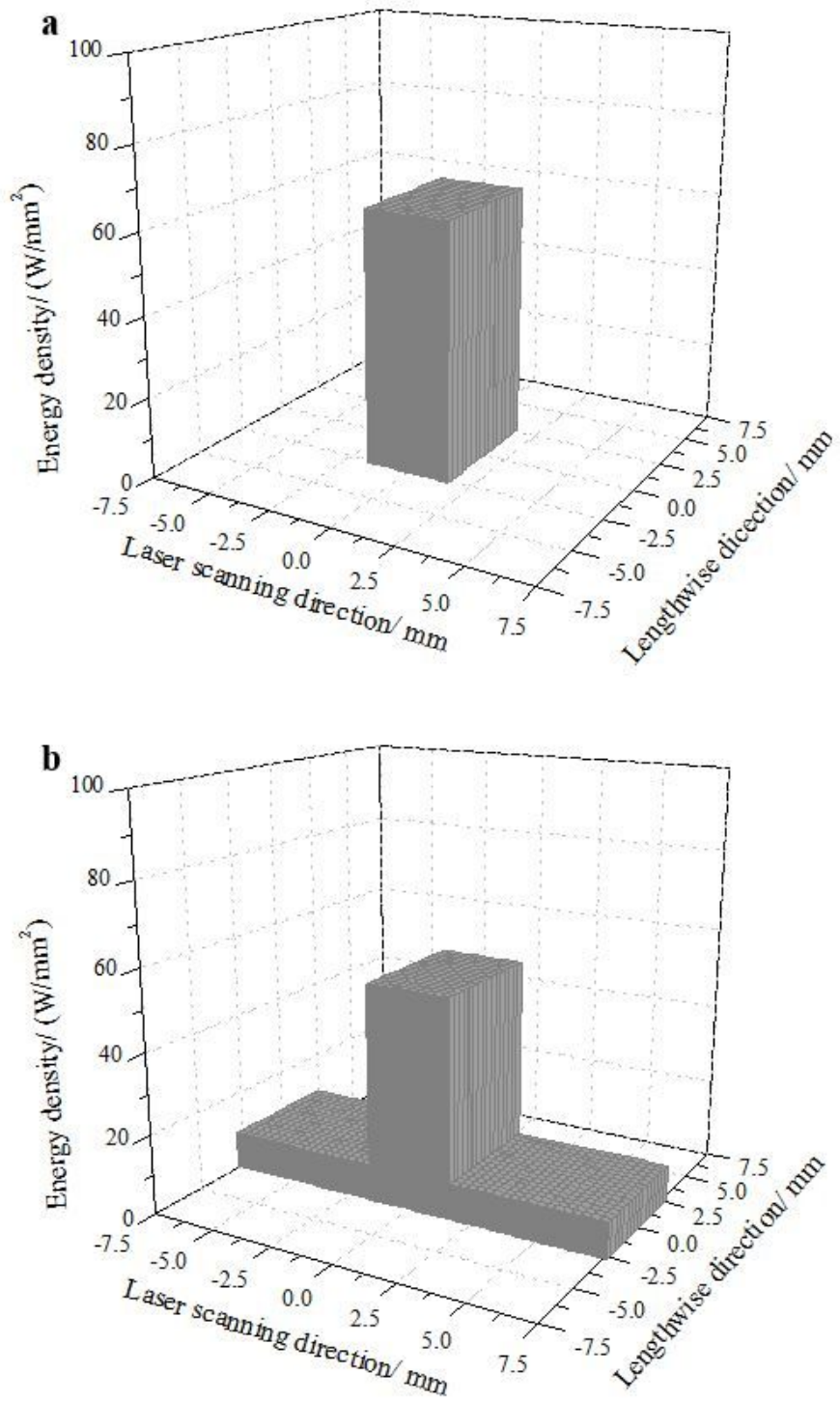

Figure 2

Energy density distribution of laser beam spots. a uniform rectangular beam spot, b convex shape beam spot

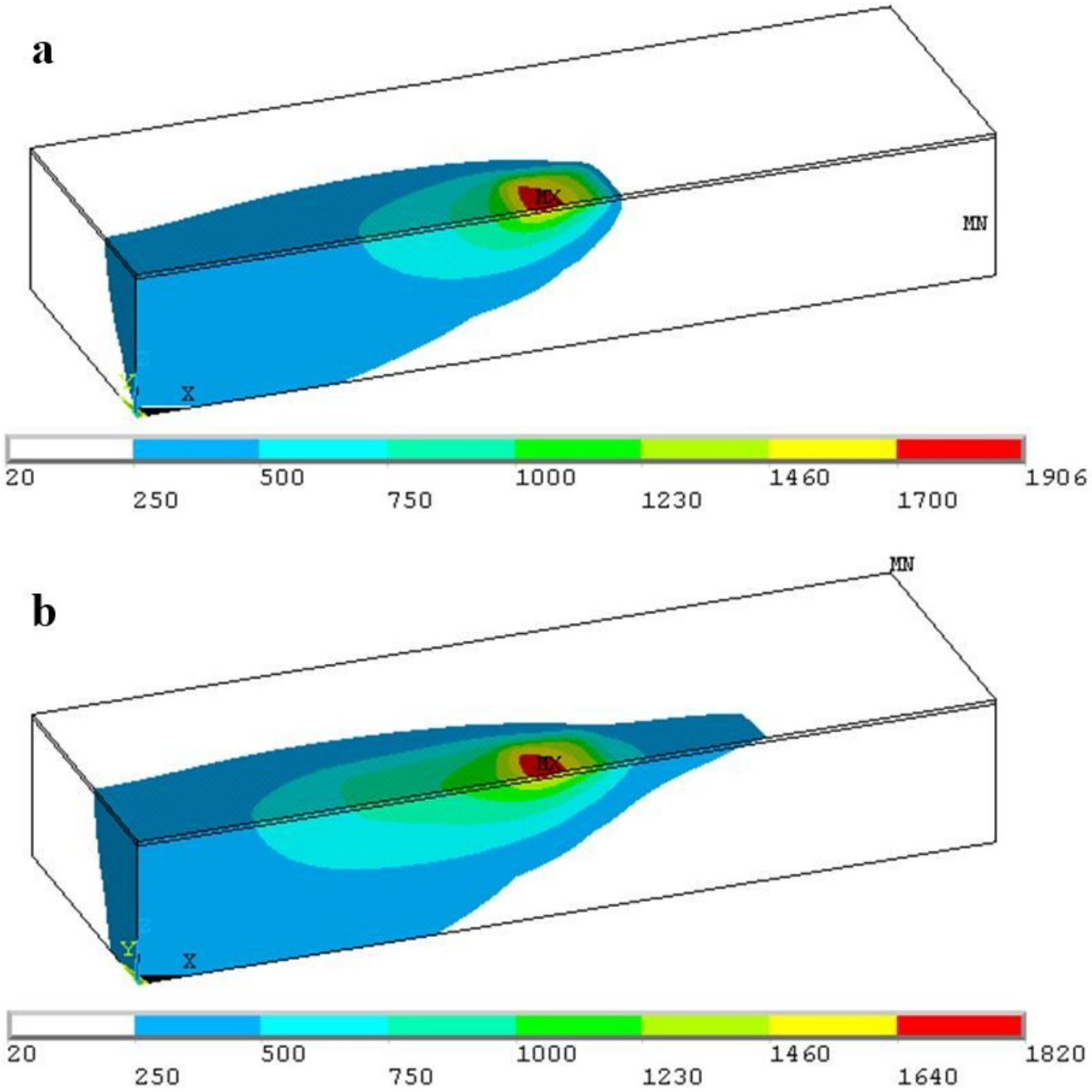

Figure 3

Temperature field nephogram at 1.5 s. a uniform rectangular beam spot, b convex shape beam spot

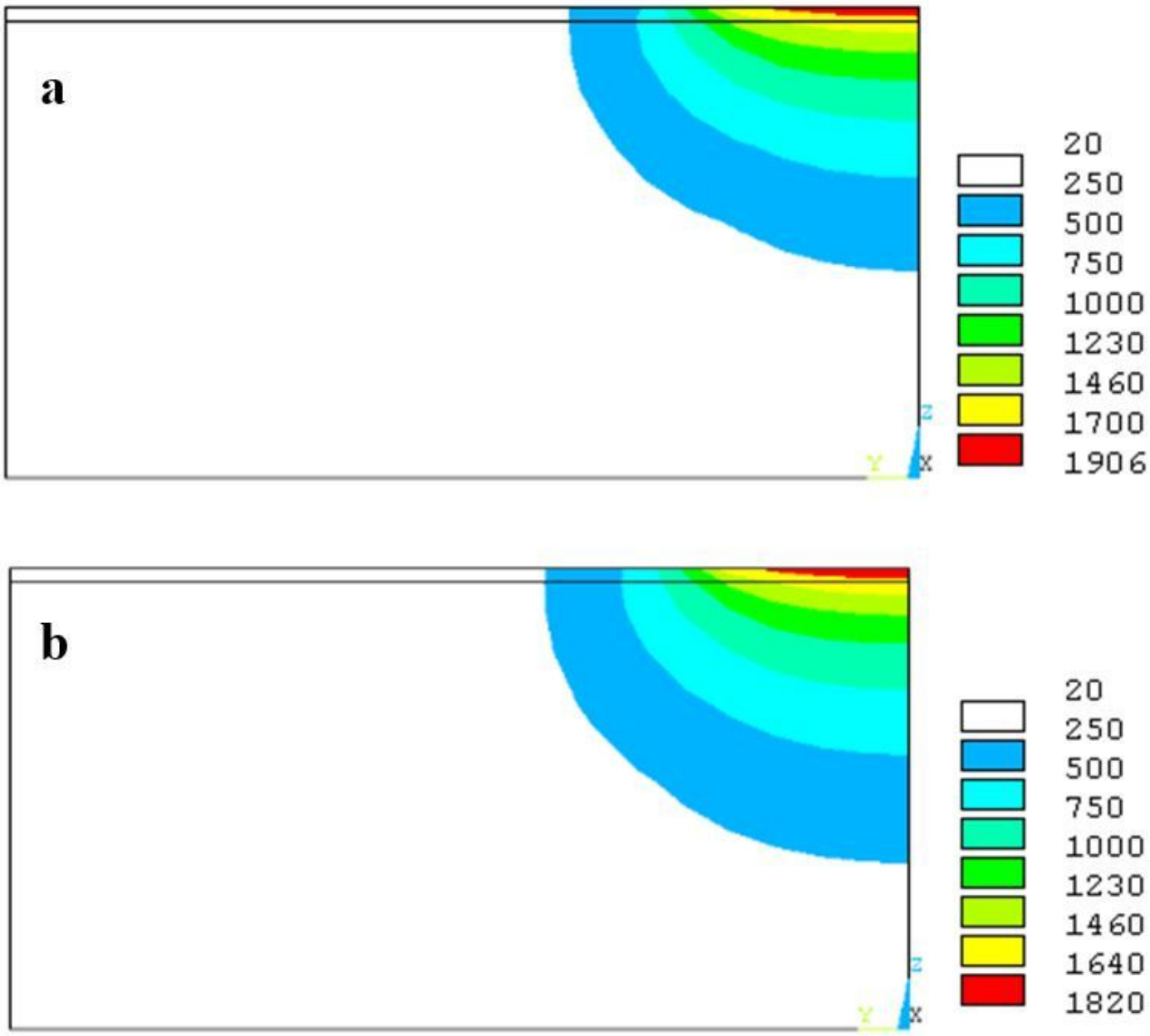

Figure 4

Cross-sectional temperature field nephogram of the maximum temperature point at 1.5 s. a uniform rectangular beam spot, b convex shape beam spot

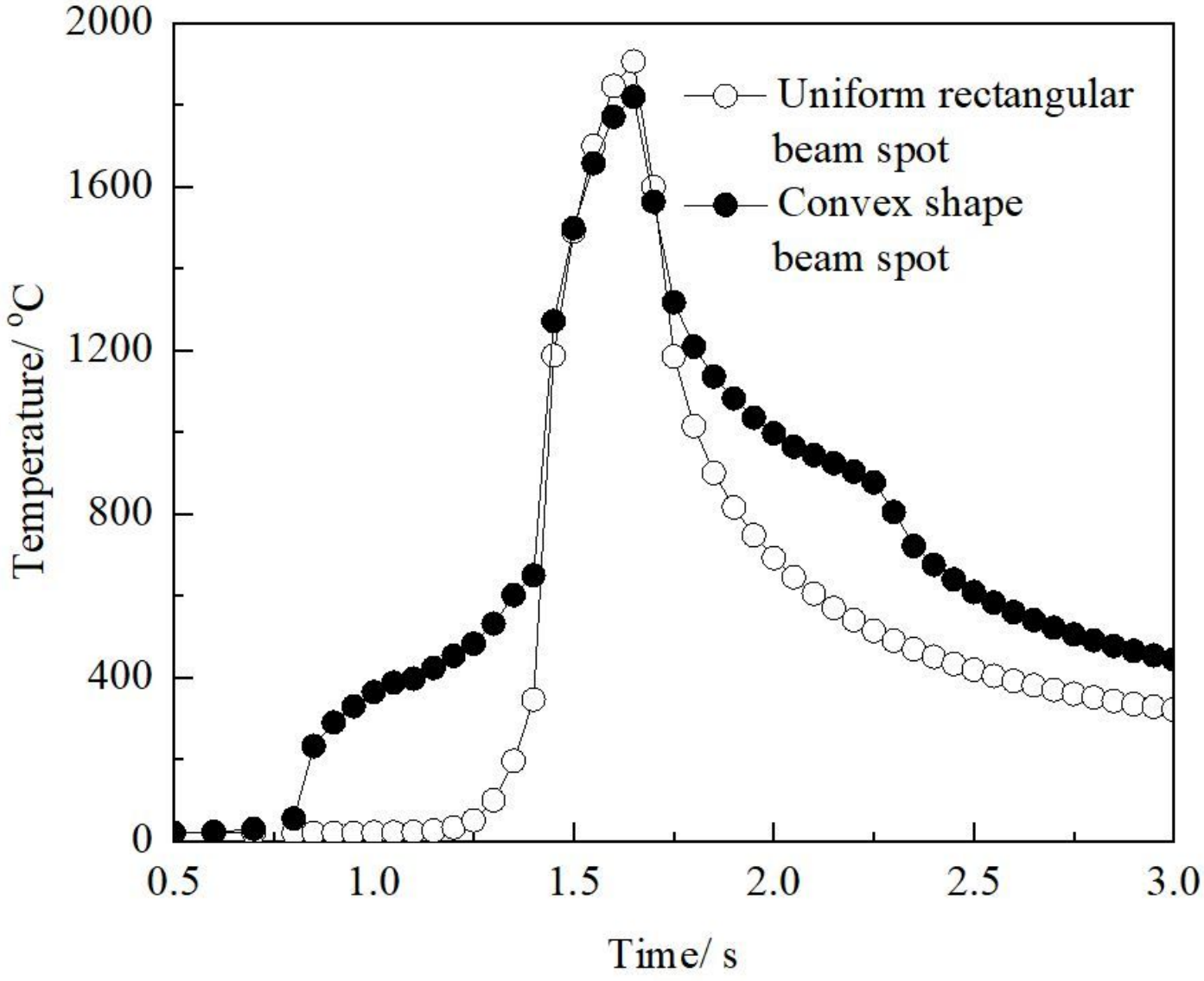

Figure 5

Thermal cyclic curves of midpoint of laser scanning center line on upper surface

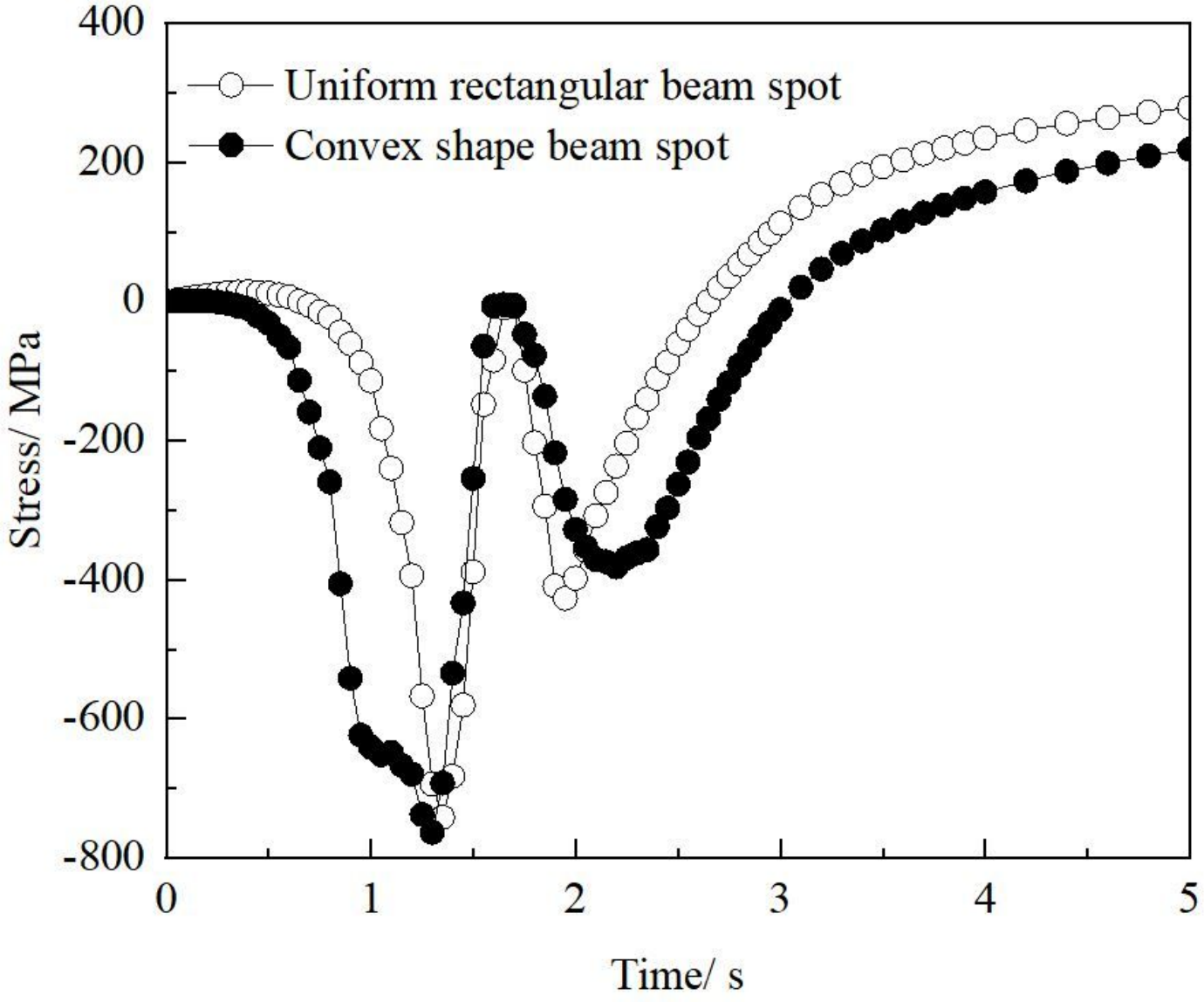

Figure 6

Stress cyclic curves of midpoint of laser scanning center line on upper surface

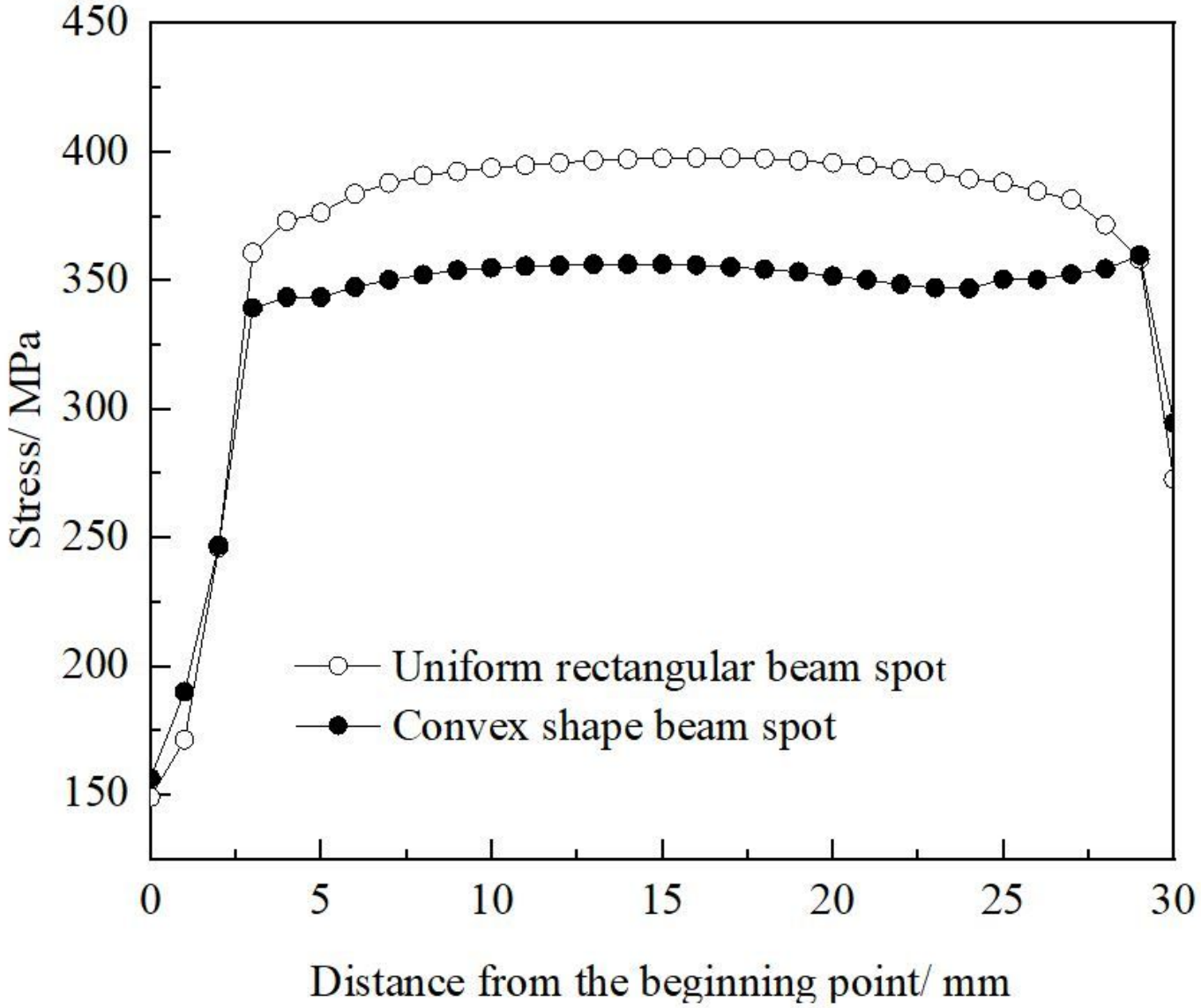

Figure 7

Residual stress distribution on laser scanning center line on upper surface

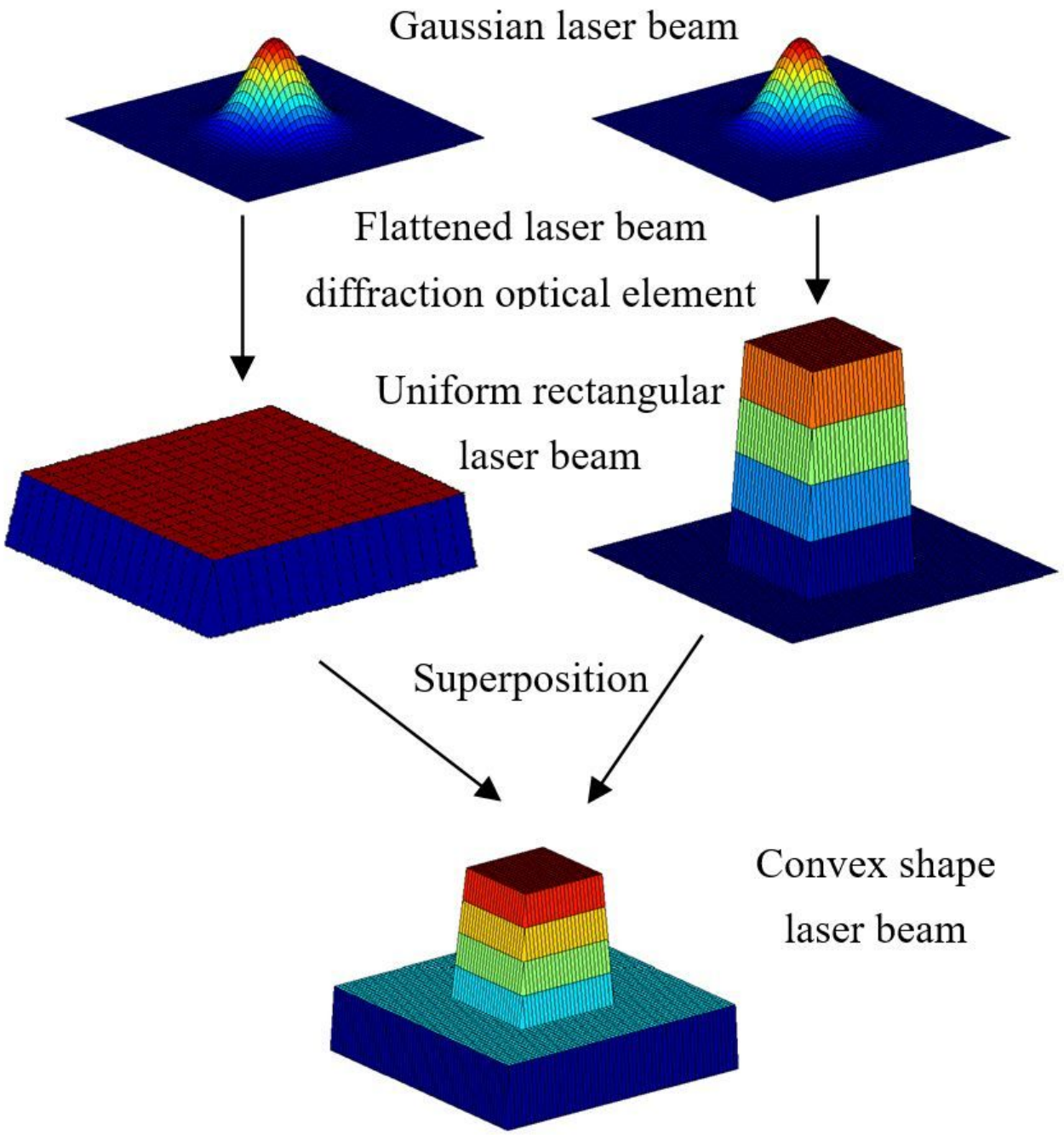

Figure 8

Schematic diagram of convex shape beam spot generation through double-beam superposition of uniform rectangular beam spot